

Electronic Supplementary Information

Experimental Section

Materials: All chemicals are purchased and used without further purification.

Sodium hydroxide (NaOH), ethylalcohol (C₂H₅OH), hydrochloric acid (HCl), Sulfuric acid (H₂SO₄) were bought from Beijing Chemical Co., Ltd (China). Ethylene glycol (EG, 95%) was purchased from Shanghai Hushi Reagent Co., Ltd., Deionized water (18 MΩ). Chloroiridic acid (H₂IrCl₆, 35%) was purchased from Shanghai Leyan Reagent Co., Ltd. Titanium plate (TP) (thickness is 0.2 mm) was purchased from Qingyuan Metal Materials Co., Ltd (Xingtai, China.). Carbon Paper (CP) (39BB) was purchased from Suzhou Sinero Technology Co., Ltd. Iridium oxide (IrO₂) was purchased from Aladdin Ltd. (Shanghai, China). All reagents used in this work were of analytical grade.

Preparation of TiO₂/TP: Firstly, TP was cut into a small piece (3.0 × 1.0 cm²) and sonicated in ethanol, and distilled water for 15 min, respectively. After then, TP was put into 10 M NaOH aqueous solution in 50 mL Teflon-lined autoclave. The autoclave was kept in an electric oven at 160 °C for 6 h. After the autoclave was cooled down naturally to room temperature, the sample was moved out, washed with deionized water and ethanol several times and dried at 60 °C for 60 min. Then the resultant Na-titanate/TP was immersed in 0.1 M HCl for 4 h to exchange Na⁺ with H⁺, followed by rinsing several times with deionized water and then dried at 60 °C. Subsequently, the prepared H₂Ti₂O₃/TP was cut into 1.0×1.0 cm² pieces prior to be annealed in H₂/Ar atmosphere at 700 °C for 3 h, After cooling to room temperature, TiO₂/TP was finally obtained.

Preparation of Ir-TiO₂/TP: Subsequently, the prepared TiO₂/TP was soaked in a fully dispersed Chloroiridic-EG solution (3 μL of chloroiridic acid is uniformly dispersed in 10 mL of ethylene glycol) for 30min, then, put it in a 20 mL Teflon-lined autoclave. The autoclave was kept in an electric oven at 120 °C for 12 h, After the autoclave was cooled down to room temperature, the sample was moved out, washed with deionized water and ethanol several times and dried at 60 °C for 1d, Ir-TiO₂/TP was finally obtained.

Preparation of IrO₂ electrode: 4 mg of the catalyst (commercial IrO₂) was dispersed in a mixture of 480 μL of isopropanol and 20 μL of Nafion solution. The mixture was sonicated for 60 minutes to

form a homogeneous ink. 250 μ L of the catalyst ink was drop-casted onto a carbon paper (CP) and dried at room temperature, with a loading mass of 2 mg cm^{-2} .

Characterizations: The crystal structure of as-prepared materials was identified through X-ray diffraction (XRD, Philip D8). Raman spectroscopy was conducted on a Jobin-Yvon LabRAM HR-800 spectrometer with a laser excitation at 532 nm. Scanning electron microscopy (SEM, ZISS 300) and transmission electron microscopy (TEM, JEM-F200, JEOL Ltd.) were carried out to reveal the morphology information of samples. Energy dispersive X-ray (EDX) and X-ray photoelectron spectroscopy (XPS, ESCALAB 250 Xi) were utilized to analyze chemical compositions.

Electrochemical measurements: All electrochemical measurements were conducted on a Gamry Interface5000E electrochemical workstation (USA). The Ir-TiO₂/TP electrode ($1 \times 1 \text{ cm}^2$) served as the working electrode, with a platinum electrode as the counter electrode and an MSE electrode (Hg-Hg₂SO₄) as the reference electrode. The electrolyte used was a 0.5 M H₂SO₄ solution. The OER performance of the Ir-TiO₂/TP electrode was evaluated in the 0.5 M H₂SO₄ electrolyte and compared with that of TiO₂/TP and IrO₂ on CC. Unless otherwise specified, electrochemical data were normalized and reported based on the geometric area of the electrode. Prior to data acquisition, all electrodes underwent electrochemical activation through multiple cyclic voltammetry scans until a stable state was reached. The measurements were performed at room temperature using a standard three-electrode setup without stirring. Polarization curves were obtained via linear sweep voltammetry (LSV) at a scan rate of 0.005 V s^{-1} with IR compensation (100%). Electrochemical impedance spectroscopy (EIS) was conducted at a potential corresponding to 15 mA cm^{-2} , with a frequency range of 1 Hz to 10 kHz and an amplitude of 10 mV. Different scan rates were employed during the cyclic voltammetry measurements to get the double-layer capacitance value (C_{dl}), and the current density (Janodic-Jscodic) at the midpoint of the scan voltage interval was found to be linearly related to the scan rate. All potentials reported in our work were converted to the reversible hydrogen electrode (RHE) using the following equation:

$$E(\text{RHE}) = E(\text{Hg}_2\text{SO}_4) + 0.0592 \times \text{pH} + 0.656 \text{ V} \quad (1)$$

and the current density was normalized to the geometric surface area.

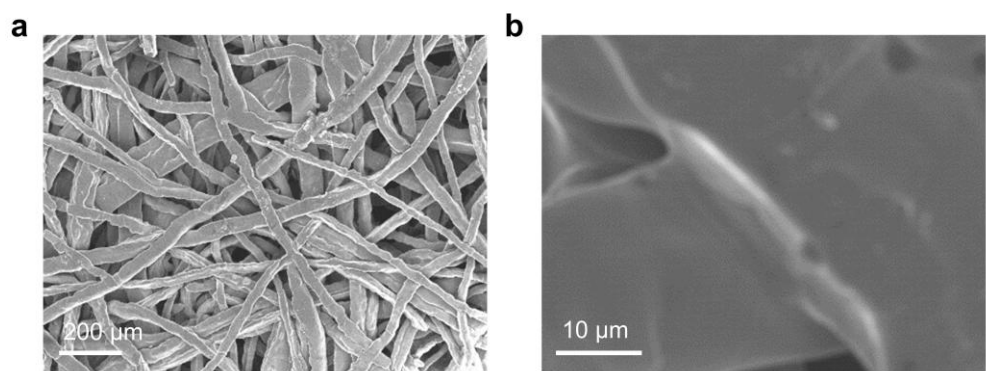


Fig. S1. SEM image of bare TP (a)85x, (b)2200x

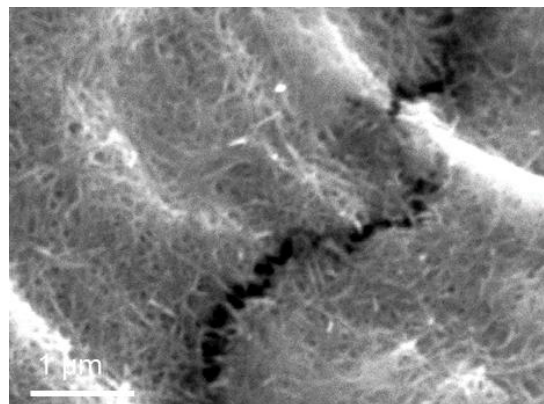


Fig. S2. SEM image of $\text{Na}_2\text{TiO}_3/\text{TP}$

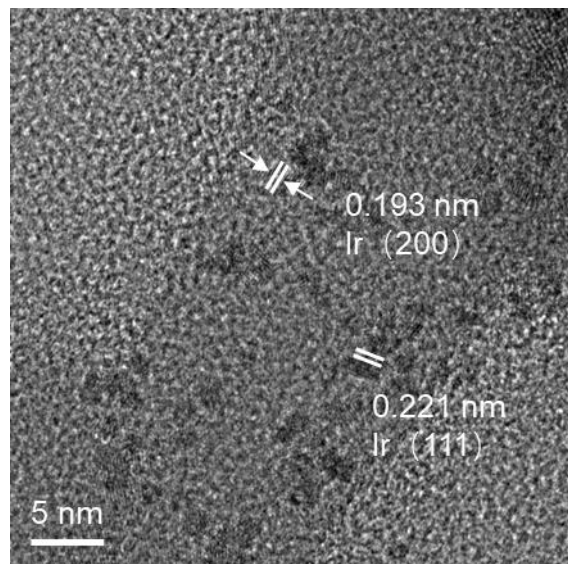


Fig. S3. HR-TEM image of Ir-TiO₂/TP.

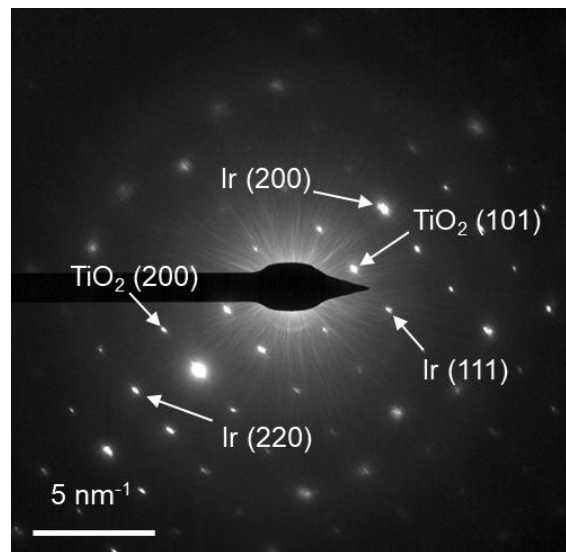


Fig. S4. SAED pattern of Ir-TiO₂/TP.

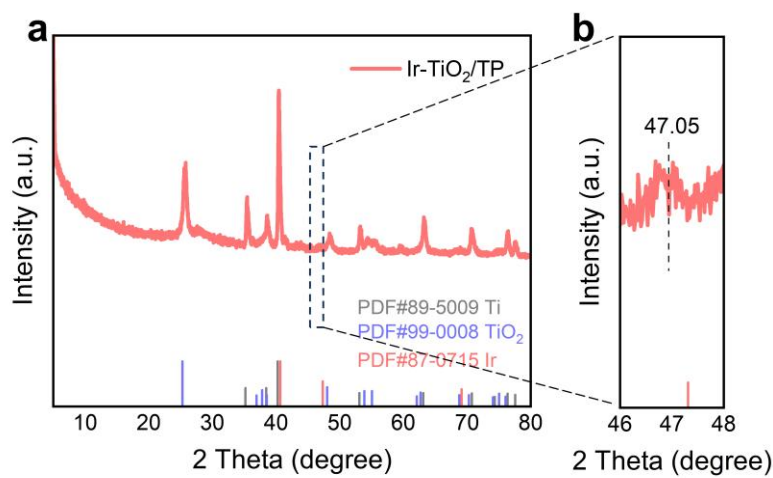


Fig. S5. (a) XRD patterns of Ir-TiO₂/TP, (b) Partial enlarged XRD patterns of Ir-TiO₂/TP.



Fig. S6. The electrochemical device for OER performance test.

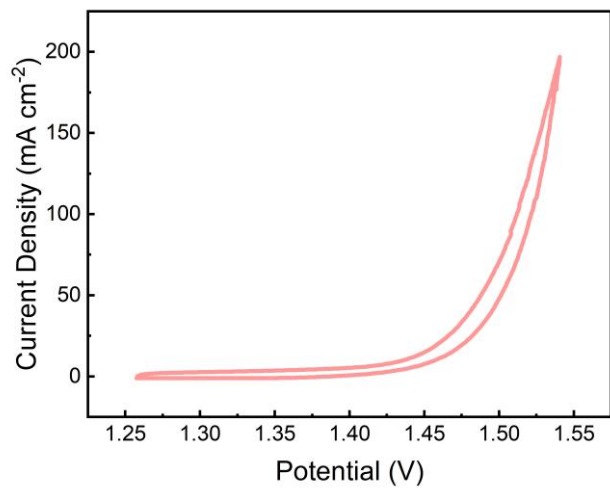


Fig. S7. CV curve of Ir-TiO₂/TP in 0.5 M H₂SO₄.

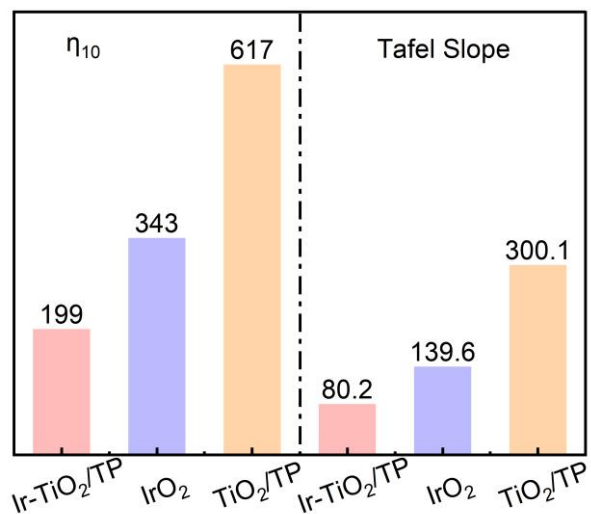


Fig. S8. Comparison of overpotential and Tafel slope between Ir-TiO₂/TP, TiO₂/TP and IrO₂.

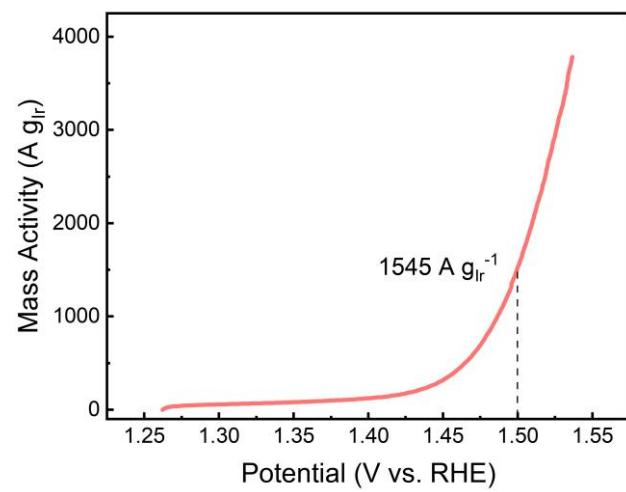


Fig. S9. Mass activities curve of Ir-TiO₂/TP.

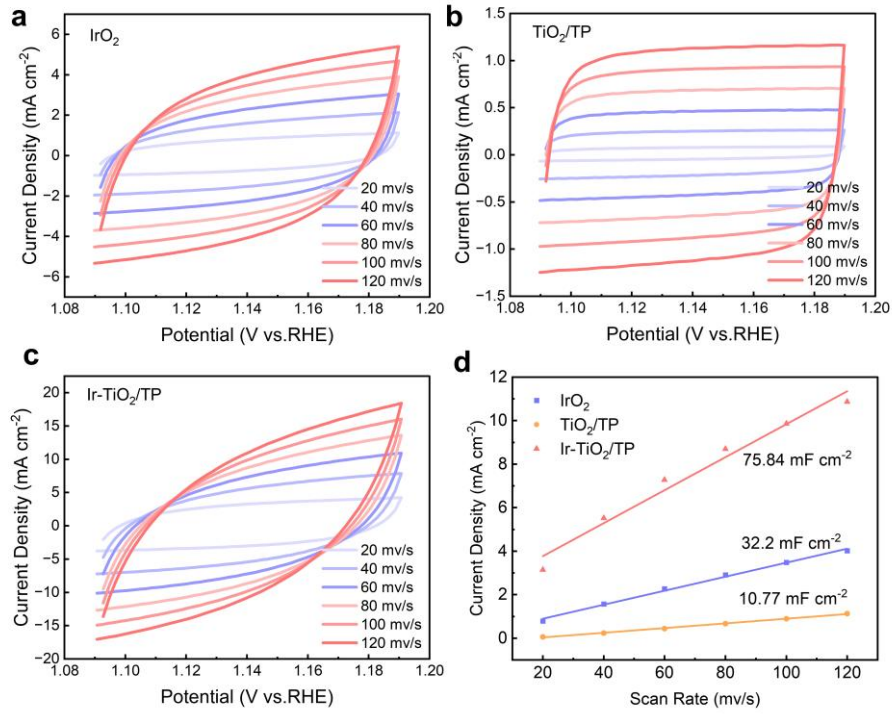


Fig. S10. Cyclic voltammograms recorded at a series of scan rates of (a) IrO_2 , (b) TiO_2/TP , (c) $\text{Ir-TiO}_2/\text{TP}$ and (d) Electrochemical double layer capacitances of TiO_2/TP , IrO_2 and $\text{Ir-TiO}_2/\text{TP}$.

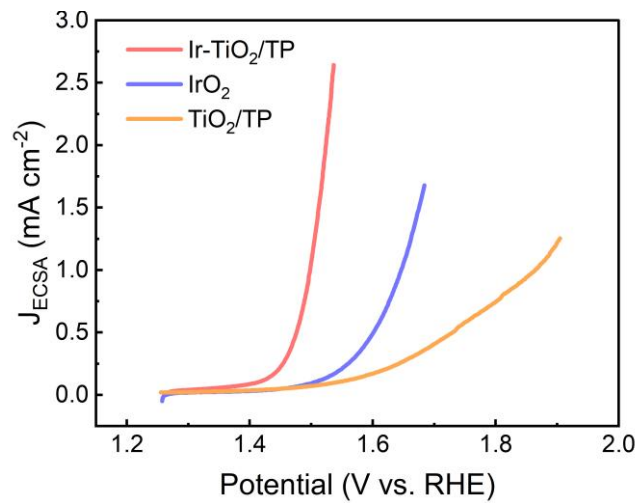


Fig. S11. ECSA-normalized LSV curves of TiO₂/TP, IrO₂ and Ir-TiO₂/TP.

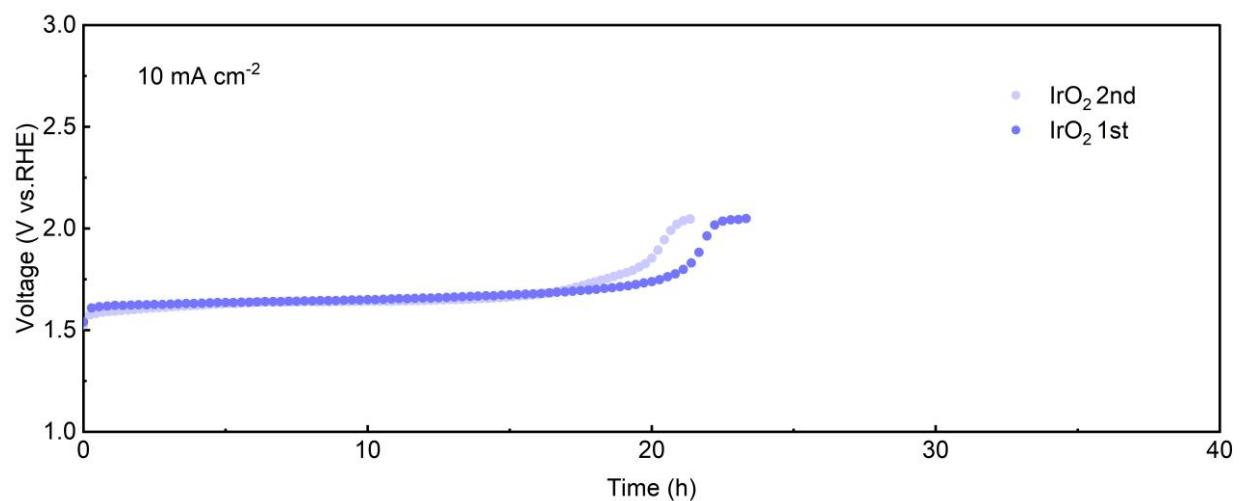


Fig. S12. The two Three-electrode stability tests for IrO₂ at 10 mA cm⁻².

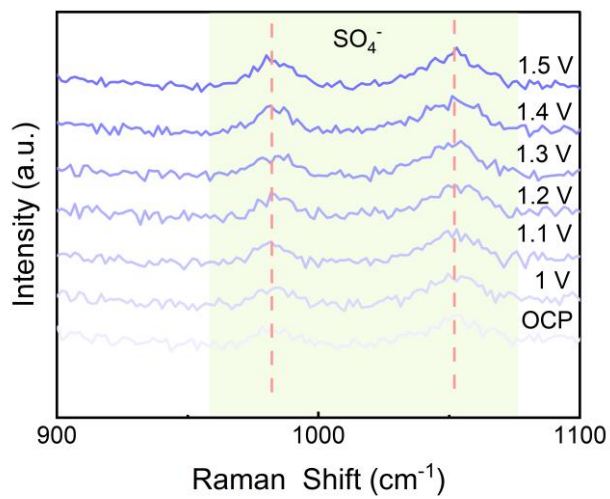


Fig. S13. The enlarged view of the in-situ Raman spectrum of Ir-TiO₂/TP in the range of 900 - 1100 cm⁻¹.

Table S1. Ir loading of the Ir-TiO₂/TP catalyst.

Catalyst Mass/g	TP Area/cm ⁻²	Ir concentration/mg L ⁻¹
0.085g	1	1.06

Tip: Ir-TiO₂/TP (1 cm²) was dissolved into a 50 mL solution for ICP testing.

Table S2. The atomic molar ratios of elements from the XPS analysis.

Element	Position (eV)	FWHM (eV)	Peak area	Atomic (%)
O	529.95	3.07	1523436.21	45.72
Ti	457.91	2.80	1630056.93	20.61
Ir	62.98	0.77	30811.30	0.14
C	284.80	2.95	461670.53	33.53

Table S3. Comparison of catalytic performance of Ir-TiO₂/TP with recently reported OER electrocatalysts in acidic electrolyte.

Catalyst	Electrolyte	electrode area (cm ²)	Ir loading (μg _{Ir} cm ⁻²)	MA (A g _{Ir} ⁻¹) (RHE)	Overpotential at 10mA cm ⁻² (mV)	Stability (h)	Reference
Ir-TiO₂/TP	0.5 M H₂SO₄	1	53	1545 @ 1.5V	199	440 @ 10 mA cm⁻²	This work
Ti/TiO ₂ NTs/IrRuOx	0.5 M H ₂ SO ₄	1	144	-	190	300h @ 10mA cm ⁻²	¹
Ti-IrOx/Ir	0.5 M H ₂ SO ₄	0.196	1400	338 @ 1.58V	254	100h @ 10mA cm ⁻²	²
Ir ₈₈ Ru ₁₂ @CMa	0.1 M HClO ₄	0.25	1000	-	229	120h @ 10mA cm ⁻²	³
857.6							
IrOx/Nb ₄ N ₅ -40	0.5 M H ₂ SO ₄	0.196	382	@ 1.7 V (A g _{IrO₂} ⁻¹)	247	40h @ 10mA cm ⁻²	⁴
Ir-NCT/CC	0.1 M HClO ₄	1	5.7	6930 @ 1.49V	202	50h @ 10mA cm ⁻²	⁵
IrGa-IMC@IrOx	0.1 M HClO ₄	0.196	20	841 @ 1.52V	272	3,000 voltammetry cycles	⁶
Ir-C	0.5 M H ₂ SO ₄	0.246	40	825 @ 1.52V	256	20h @ 10mA cm ⁻²	⁷
IrOx/ATO	0.05 M H ₂ SO ₄	0.196	10.2	78 @ 1.52V	434	15 h @ 1mA cm ⁻²	⁸
DO-IrNi _{3.3}	0.05 M H ₂ SO ₄	0.196	10.2	411 @ 1.52V	310	3h @ 1 mA cm ⁻²	⁹
Ir ₄₄ Pd ₁₀	0.1 M HClO ₄	0.196	12.5	2600 @ 1.49V	226	15h @ 10 mA cm ⁻²	¹⁰
Ir-STO	0.1 M HClO ₄	0.196	210	750 @ 1.52V	247	7.5h @ 10mA cm ⁻²	¹¹
Co-RuIr	0.1 M HClO ₄	0.196	50	-	235	25h @ 10mA cm ⁻²	¹²
Ir-NSG	0.1 M HClO ₄	0.196	22	355 @ 1.52V	265	24h @ 10mA cm ⁻²	¹³

Reference

- 1 K. Lv, J. Na, J. Chi, S. Jia, H. Yu, Z. Shao, *Int. J. Hydrogen Energy*, **2024**, *60*, 825-834.
- 2 Y. Wang, R. Ma, Z. Shi, H. Wu, S. Hou, Y. Wang, C. Liu, J. Ge, W. Xing, *Chem*, **2023**, *9*, 2931-2942.
- 3 T. B. N. Huynh, J. Song, H. E. Bae, Y. Kim, M. D. Dickey, Y. E. Sung, M. J. Kim, O. J. Kwon, *Adv. Funct. Mater.*, **2023**, *33*, 2301999.
- 4 X. Duan, H. Liu, W. Zhang, Q. Ma, Q. Xu, L. Khotseng, H. Su, *Electrochim. Acta*, **2023**, *470*, 143271.
- 5 C. Yang, X. Zhang, Q. An, M. Liu, W. Zhou, Y. Li, F. Hu, Q. Liu, H. Su, *J. Energy Chem.*, **2023**, *78*, 374-380.
- 6 L.-W. Chen, F. He, R.-Y. Shao, Q.-Q. Yan, P. Yin, W.-J. Zeng, M. Zuo, L. He, H.-W. Liang, *Nano Res.*, **2021**, *15*, 1853-1860.
- 7 Y. Peng, Q. Liu, B. Lu, T. He, F. Nichols, X. Hu, T. Huang, G. Huang, L. Guzman, Y. Ping, S. Chen, *ACS Catal.*, **2021**, *11*, 1179-1188.
- 8 H.-S. Oh, H. N. Nong, T. Reier, A. Bergmann, M. Gliech, J. Ferreira de Araújo, E. Willinger, R. Schlögl, D. Teschner, P. Strasser, *J. Am. Chem. Soc.*, **2016**, *138*, 12552-12563.
- 9 H. N. Nong, L. Gan, E. Willinger, D. Teschner, P. Strasser, *Chem. Sci.*, **2014**, *5*, 2955-2963.
- 10 J. Zhu, Z. Chen, M. Xie, Z. Lyu, M. Chi, M. Mavrikakis, W. Jin, Y. Xia, *Angew. Chem. Int. Ed.*, **2019**, *58*, 7244-7248.
- 11 X. Liang, L. Shi, Y. Liu, H. Chen, R. Si, W. Yan, Q. Zhang, G. D. Li, L. Yang, X. Zou, *Angew. Chem. Int. Ed.*, **2019**, *58*, 7631-7635.
- 12 J. Shan, T. Ling, K. Davey, Y. Zheng, S. Z. Qiao, *Adv. Mater.*, **2019**, *31*, 1900510.
- 13 Q. Wang, C.-Q. Xu, W. Liu, S.-F. Hung, H. Bin Yang, J. Gao, W. Cai, H. M. Chen, J. Li, B. Liu, *Nat. Commun.*, **2020**, *11*, 4246.